Electronic Supplementary Material (ESI) for Journal of Materials Chemistry A.

Supplementary Information

for

Doped MXene Combinations as Highly Efficient Bifunctional and Multifunctional Catalysts for Water Splitting and Metal-Air Batteries

Rohit Anand, Babu Ram, Muhammad Umer, Mohammad Zafari, Sohaib Umer, Geunsik Lee, and Kwang S. Kim**

Center for Superfunctional Materials, Department of Chemistry, Ulsan National Institute of Science and Technology (UNIST), 50 UNIST-gil, Ulsan 44919, South Korea

*E-mail**:** gslee@unist.ac.kr**,** kimks@unist.ac.kr

Supplementary Note:

The chemical potential of the H^+ and e^- pair can be replaced by $1/2H_2(g)$ as these two are in equilibrium at standard conditions. Since it is difficult to extract exact free energy of intermediates in solution, the approximate adsorption free energy is calculated relative to the amount of H_2O and H_2 in the gas phase, defined as:

$$\begin{aligned}\Delta G_{O^*} &= \Delta G\left(H_2O(g) + * \rightarrow O^* + H_2(g)\right)\\ &= \mu_{O^*} + \mu_{H_2} - \mu_{H_2O} - \mu_*\\ &= \Big(\left(E_{O^*} + E_{H_2} - E_{H_2O} - E_*\right) + \left(E_{ZPE(O^*)} + E_{ZPE(H_2)} - E_{ZPE(H_2O)} - E_{ZPE(*)}\right) - T\\ &\quad \times \left(S_{O^*} + S_{H_2} - S_{H_2O} - S_*\right)\Big)\end{aligned}$$

$$\begin{aligned}\Delta G_{OH^*} &= \Delta G\left(H_2O(g) + * \rightarrow OH^* + 1/2H_2(g)\right)\\ &= \mu_{OH^*} + 0.5\mu_{H_2} - \mu_{H_2O} - \mu_*\\ &= \Big(\left(E_{OH^*} + 0.5E_{H_2} - E_{H_2O} - E_*\right) + \left(E_{ZPE(OH^*)} + 0.5E_{ZPE(H_2)} - E_{ZPE(H_2O)} - E_{ZPE(*)}\right)\\ &\quad - T \times \left(S_{OH^*} + S_{0.5\times H_2} - S_{H_2O} - S_*\right)\Big)\end{aligned}$$

$$\begin{aligned}\Delta G_{OOH^*} &= \Delta G\left(2H_2O(g) + * \rightarrow OOH^* + 3/2H_2(g)\right)\\ &= \mu_{OOH^*} + 1.5\mu_{H_2} - 2\mu_{H_2O} - \mu_*\\ &= \Big(\left(E_{OOH^*} + 1.5E_{H_2} - 2E_{H_2O} - E_*\right)\\ &\quad + \left(E_{ZPE(OOH^*)} + 1.5E_{ZPE(H_2)} - 2E_{ZPE(H_2O)} - E_{ZPE(*)}\right) - T\\ &\quad \times \left(S_{OOH^*} + 1.5S_{H_2} - 2S_{H_2O} - S_*\right)\Big)\end{aligned}$$

$$\begin{aligned}\Delta G_{H^*} &= \Delta G(H^+ + e^- \ * \rightarrow H^*)\\ &= \mu_{H^*} - \mu_{H^+} - \mu_{e^-} - \mu_*\end{aligned}$$

$$= \left(\left(E_{H^*} - 0.5E_{H_2} - E_*\right) + \left(E_{ZPE(H^*)} - 0.5E_{ZPE(H_2)} - E_{ZPE(*)}\right) - T \times \left(S_{H^*} - 0.5S_{H_2} - S_*\right)\right)$$

The reaction free energy ($\Delta G_1, \Delta G_2, \Delta G_3, \Delta G_4$) for OER can be written in terms of adsorption free energy using the following equations:

$$\Delta G_1 = \Delta G_{OH^*}$$
$$\Delta G_2 = \Delta G_{O^*} - \Delta G_{OH^*}$$
$$\Delta G_3 = \Delta G_{OOH^*} - \Delta G_{O^*}$$
$$\Delta G_4 = 4.92 - \Delta G_{OOH^*}$$

The reaction free energy ($\Delta G_1', \Delta G_2', \Delta G_3', \Delta G_4'$) for ORR can be written in terms of adsorption free energy using the following equations:

$$\Delta G_1' = \Delta G_{OOH^*} - 4.92$$
$$\Delta G_2' = \Delta G_{O^*} - \Delta G_{OOH^*}$$
$$\Delta G_3' = \Delta G_{OH^*} - \Delta G_{O^*}$$
$$\Delta G_4' = -\Delta G_{OH^*}$$

The theoretical overpotential for OER, ORR, and HER are calculated using the following equations:

$$\eta^{OER} = \max(\Delta G_1, \Delta G_2, \Delta G_2, \Delta G_4)/e - 1.23$$
$$\eta^{ORR} = \max(\Delta G_1', \Delta G_2', \Delta G_3', \Delta G_4')/e + 1.23$$
$$\eta^{HER} = -|\Delta G_{H*}|/e$$

Machine Learning descriptors and models

In this section, we report the explored descriptors for the classification of MXene combinations into good and bad catalysts for HER/OER/ORR. We searched for the features containing geometric, atomic, and intrinsic factors. Since we have considered $M_2M'X_2O_2$ type out-of-plane

MXene combinations for our study, the features based on M and M′ properties have abbreviation 1 and 2, respectively. The considered features are atomic number (Z1 and Z2), valence d-electrons (DE1 and DE2), first ionization energy (IE1 and IE2), Pauling electronegativity (EN1 and EN2), electron affinity (EA1 and EA2), melting point (MP1 and MP2), boiling point (BP1 and BP2), metallic radius (RC1 and RC2), metal van der Waal's radius (RV1 and RV2), and density (D1 and D2). In addition, we also considered DFT-based features: distance between adsorbed O, OH, and OOH and doped TM (namely d-O, d-OH, and d-OOH), respectively. Also, we considered distance between doped TM and adjacent surface oxygen (d-SO), distance between two surface adjacent oxygen close to the active site (d-SO2), embedding energy (Ee), difference between embedding and cohesive energy (E-C), and distance between doped TM and hydrogen (d-h).

The considered machine learning algorithms: Random Forest (RF), Gradient Boosting (GB), Support Vector classification (SVC), Bagging (BG), Naïve Bayes (NB), CatBoost (CB), Decision Tree (DT), k-nearest neighbors (KNN), Adaboost (AB), and Logistic Regression. The Pearson correlation matrix is plotted for feature selection, the features with high correlation (Pearson correlation coefficient > 0.7) are neglected and the features showing high correlation with the target are considered. In addition, the feature importance of reduced features is explored to understand the most contributing features in the best performing models for HER/OER/ORR. The confusion matrix also known as error matrix visualizes and summarizes the performance of classification algorithm. In our results, it shows the percentage of actual levels predicted correctly.

Supplementary Figures:

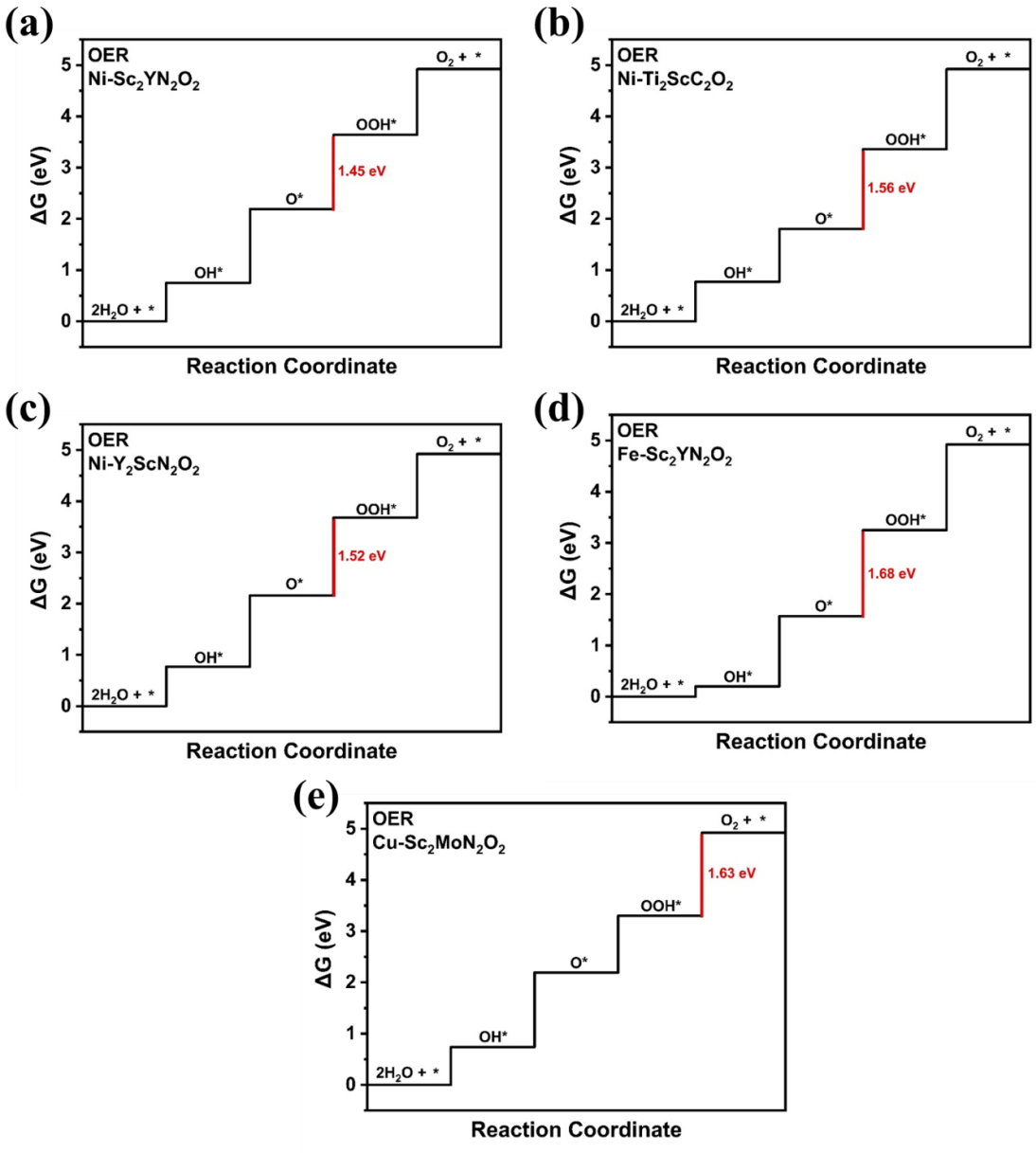

Fig. S1 Free energy diagrams of good OER catalysts **a)** Ni-$Sc_2YN_2O_2$, **b)** Ni-$Ti_2ScC_2O_2$, **c)** Ni-$Y_2ScN_2O_2$, **d)** Fe-$Sc_2YN_2O_2$, and **e)** Cu-$Sc_2MoN_2O_2$ at standard conditions. The red colored line indicates the rate-determining step for each efficient OER catalysts.

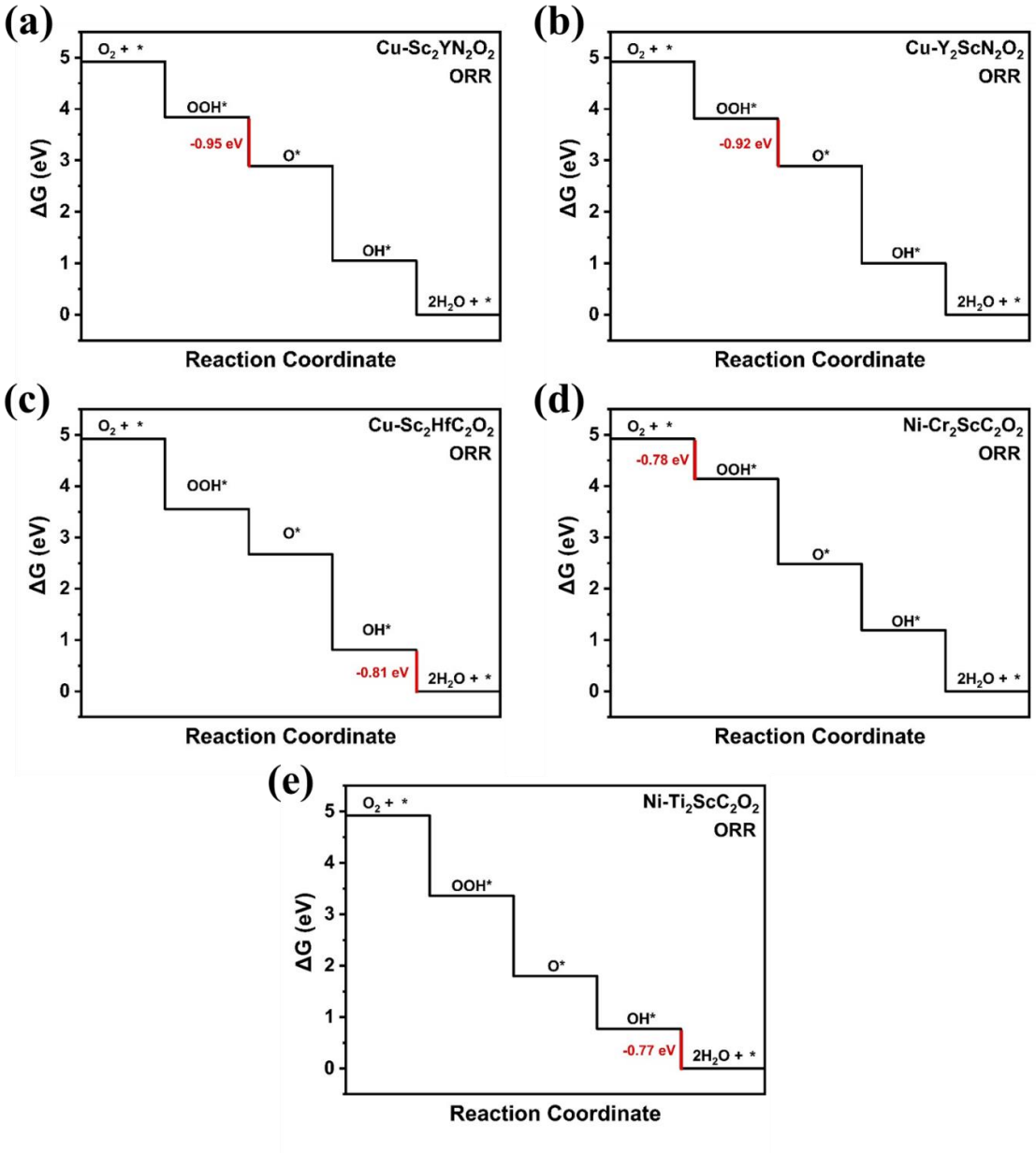

Fig. S2 Free energy diagrams of good ORR catalysts: **a)** Cu-$Sc_2YN_2O_2$, **b)** Cu-$Y_2ScN_2O_2$, **c)** Cu-$Sc_2HfC_2O_2$, **d)** Ni-$Cr_2ScC_2O_2$, and **e)** Ni-$Ti_2ScC_2O_2$ at standard conditions. The red colored line indicates the rate-determining step for each efficient ORR catalysts.

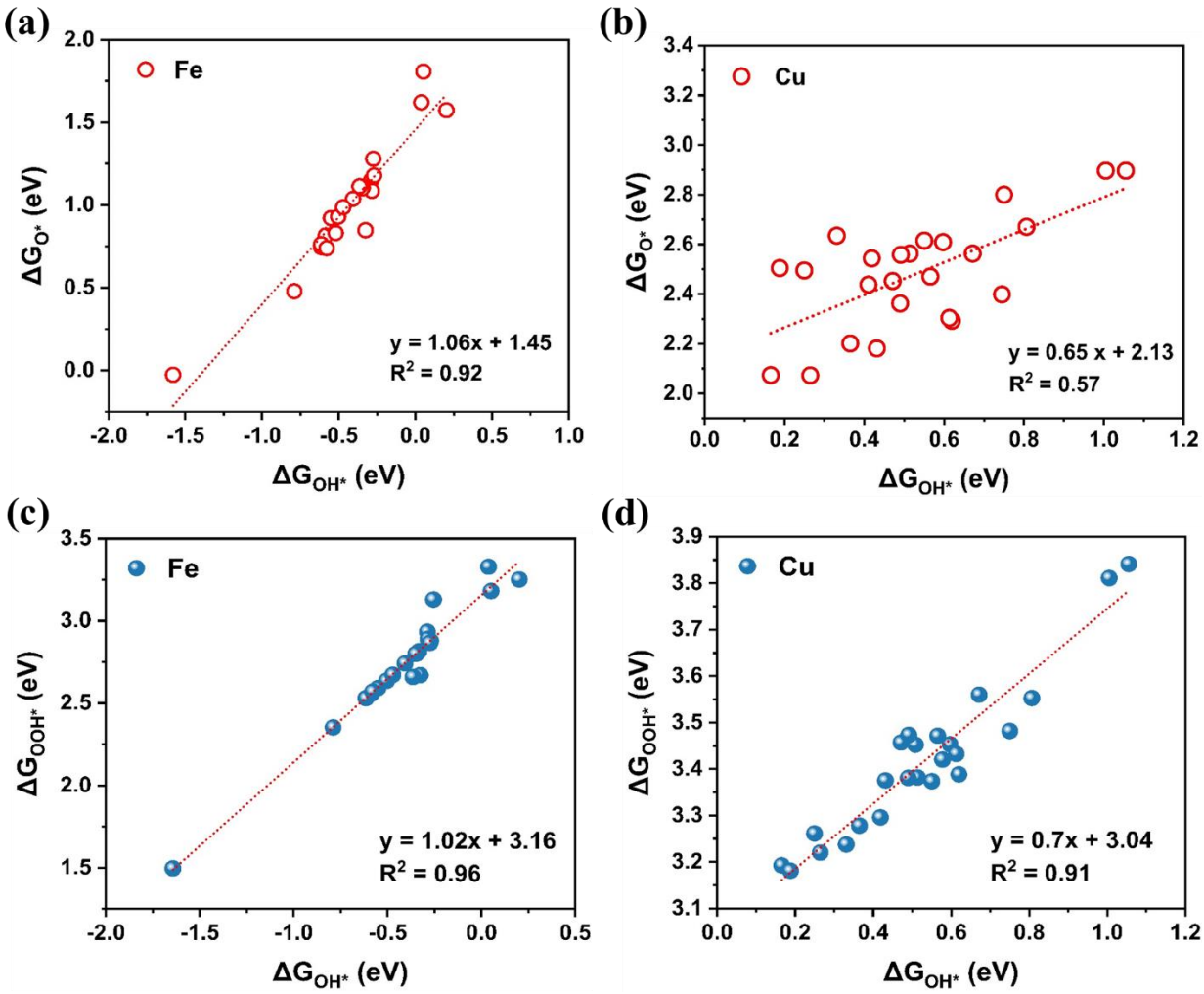

Fig. S3 The linear relationship between ΔG_{O^*} and ΔG_{OH^*} for **a)** Fe-doped, **b)** Cu-doped MXenes. The linear relationship between ΔG_{OOH^*} and ΔG_{OH^*} for **c)** Fe-doped, and **d)** Cu-doped MXenes.

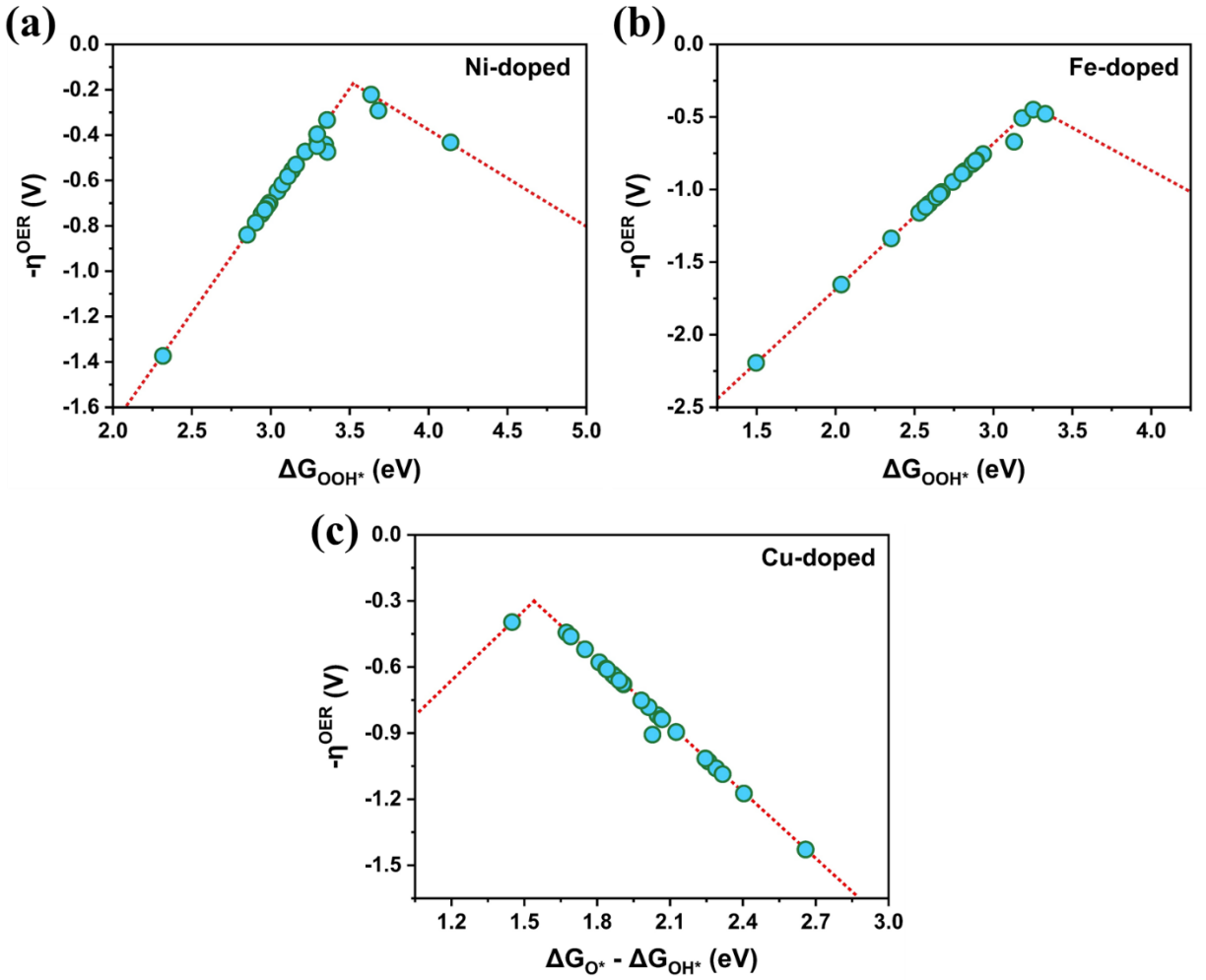

Fig. S4 Volcano plot for **a)** Ni-doped, **b)** Fe-doped, and **c)** Cu-doped MXenes between negative of OER overpotential ($-\eta^{OER}$) and ΔG_{OOH*} for Ni and Fe, and ΔG_{O*}–ΔG_{OH*} for Cu doped MXenes.

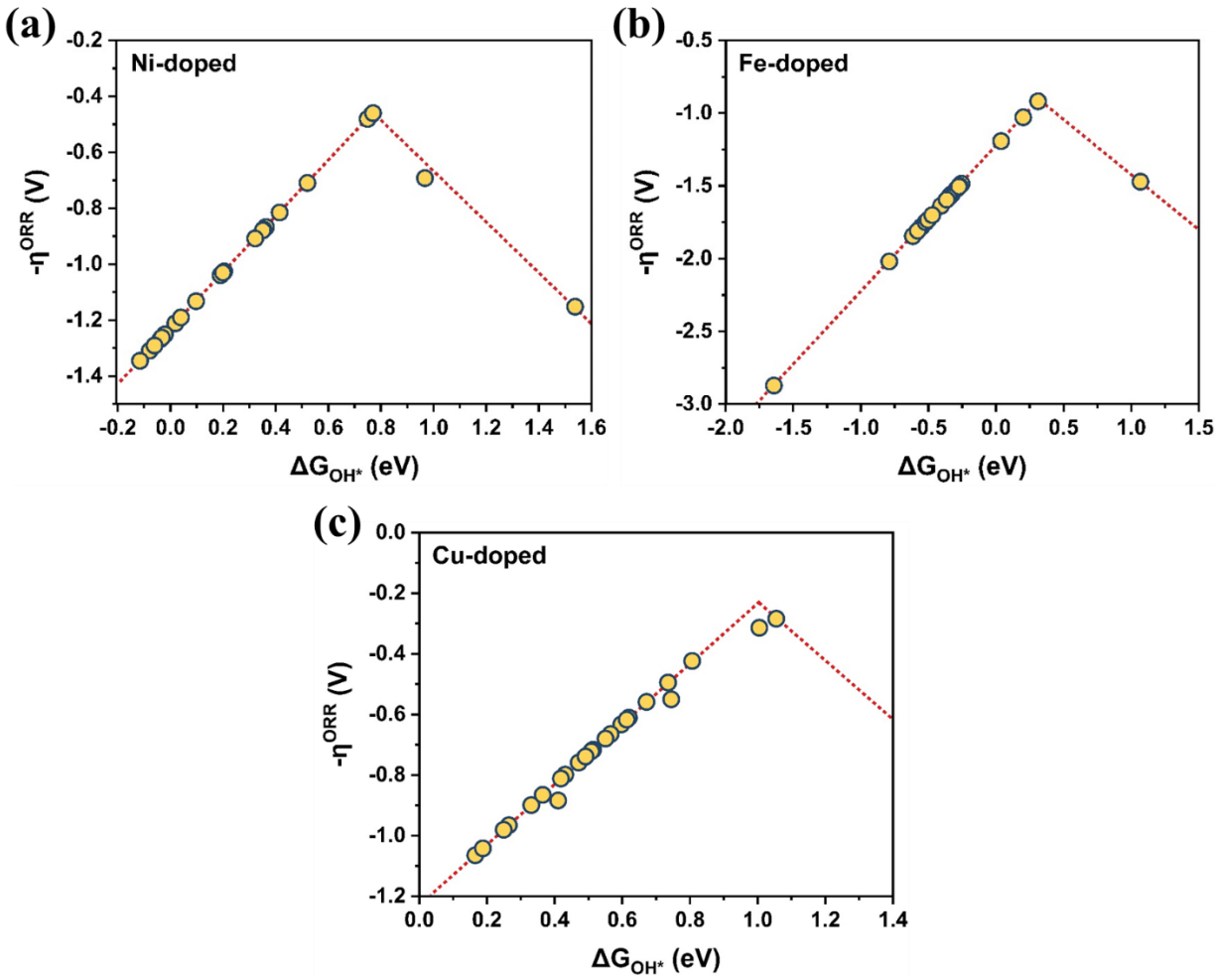

Fig. S5 Volcano plot for **a)** Ni-doped, **b)** Fe-doped, and **c)** Cu-doped MXenes between the negative value of ORR overpotential ($-\eta^{ORR}$) and ΔG_{OH*}.

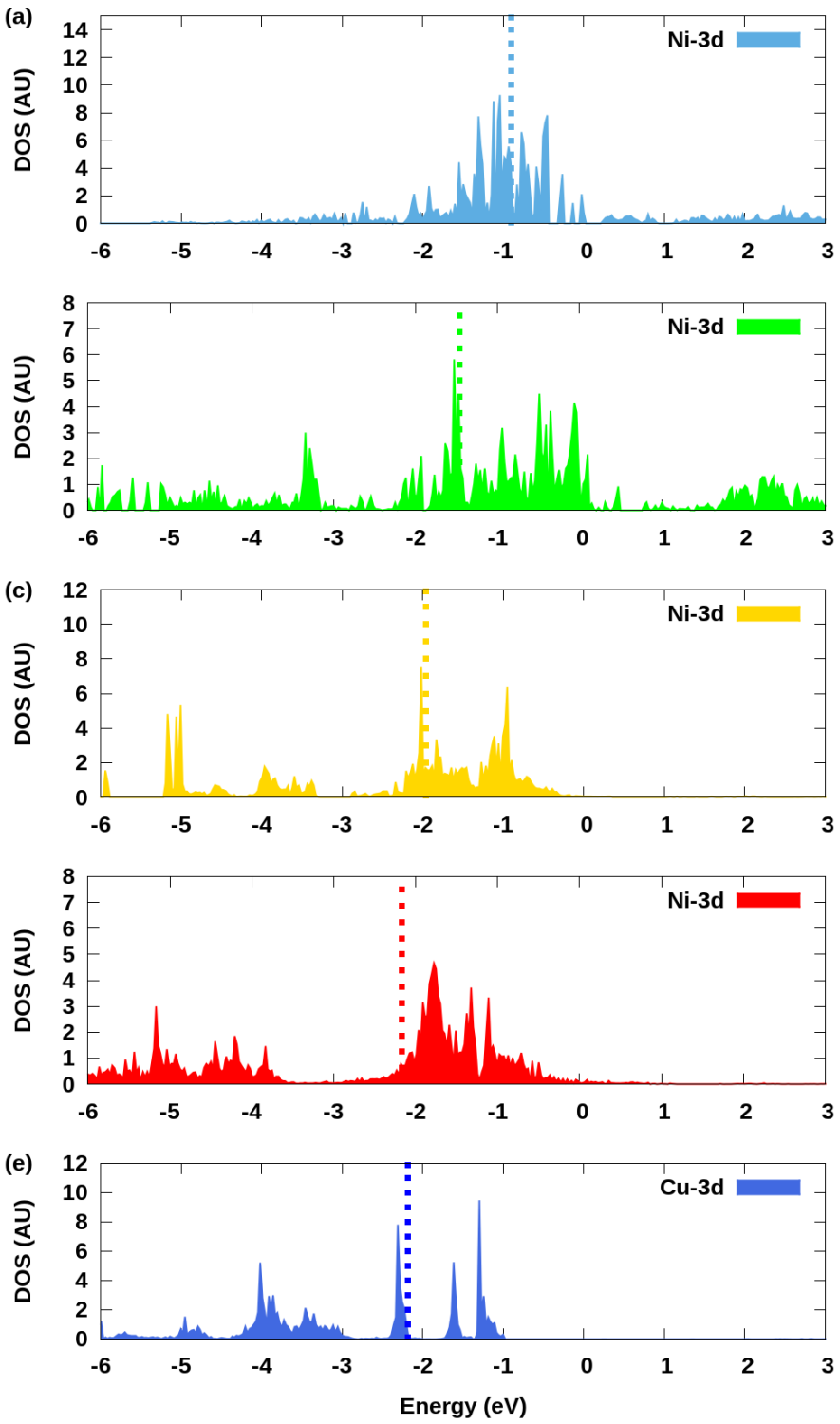

Fig. S6 The 3d states PDOS and respective d-band center (dashed lines) of doped single atom for **a)** Ni-$Sc_2YN_2O_2$, **b)** Ni-$Y_2ScN_2O_2$, **c)** Ni-$Ti_2ScC_2O_2$, **d)** Ni-$Cr_2ScC_2O_2$, and **e)** Cu-$Sc_2MoN_2O_2$. The Fermi level is set to zero.

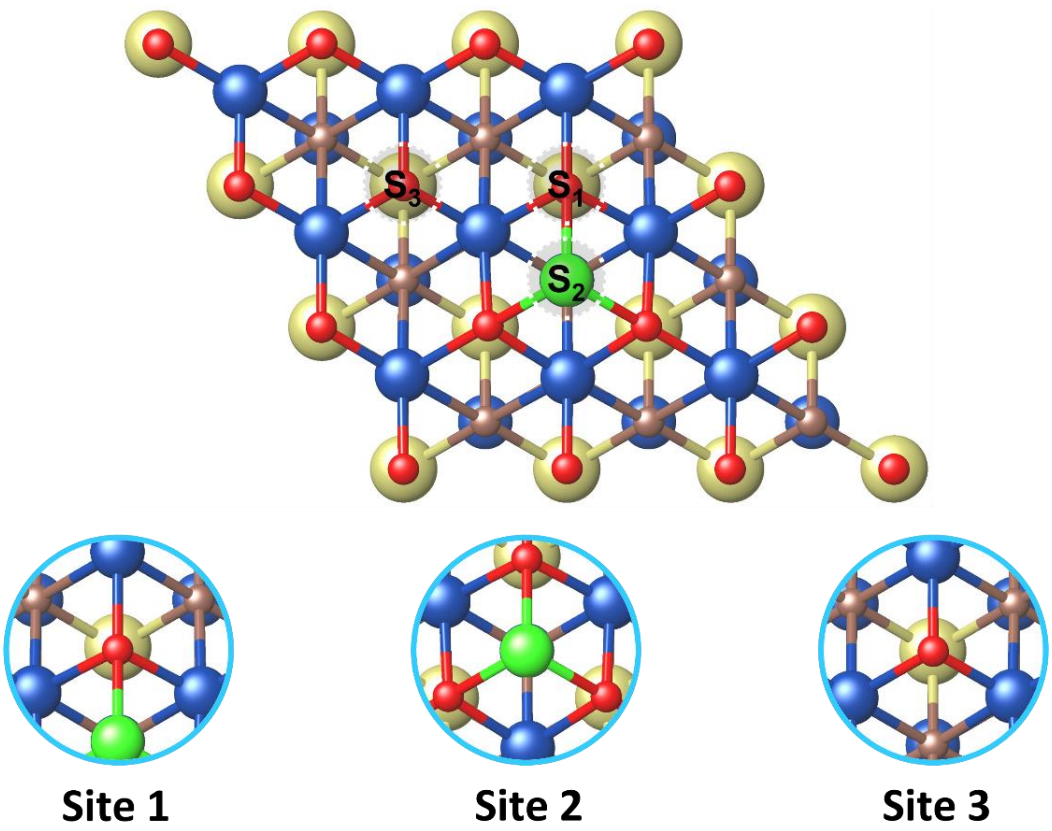

Fig. S7 Schematic top view with three different sites for H-adsorption (S_1, S_2, and S_3) for MXenes.

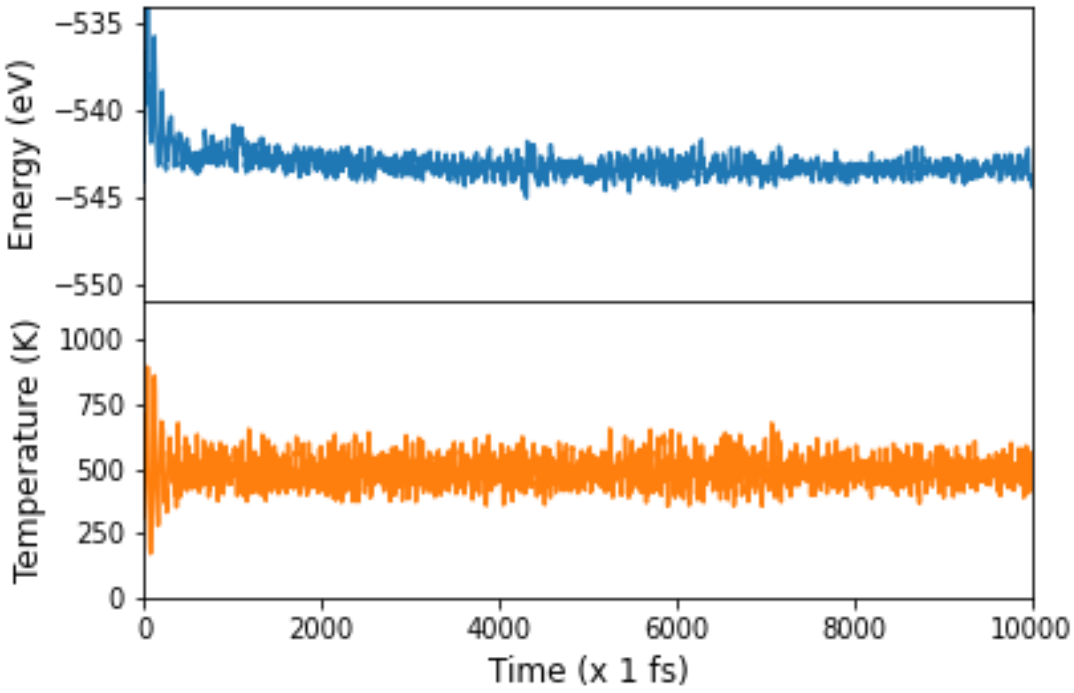

Fig. S8 The energy and temperature changes along time in MD simulation for Ni-$Cr_2ScC_2O_2$. The machine-learned potential are generated using on-the-fly sampling and sparse Gaussian regression (SGPR) algorithm as implemented in AUTOFORCE. The MD simulations are conducted at T=500K.

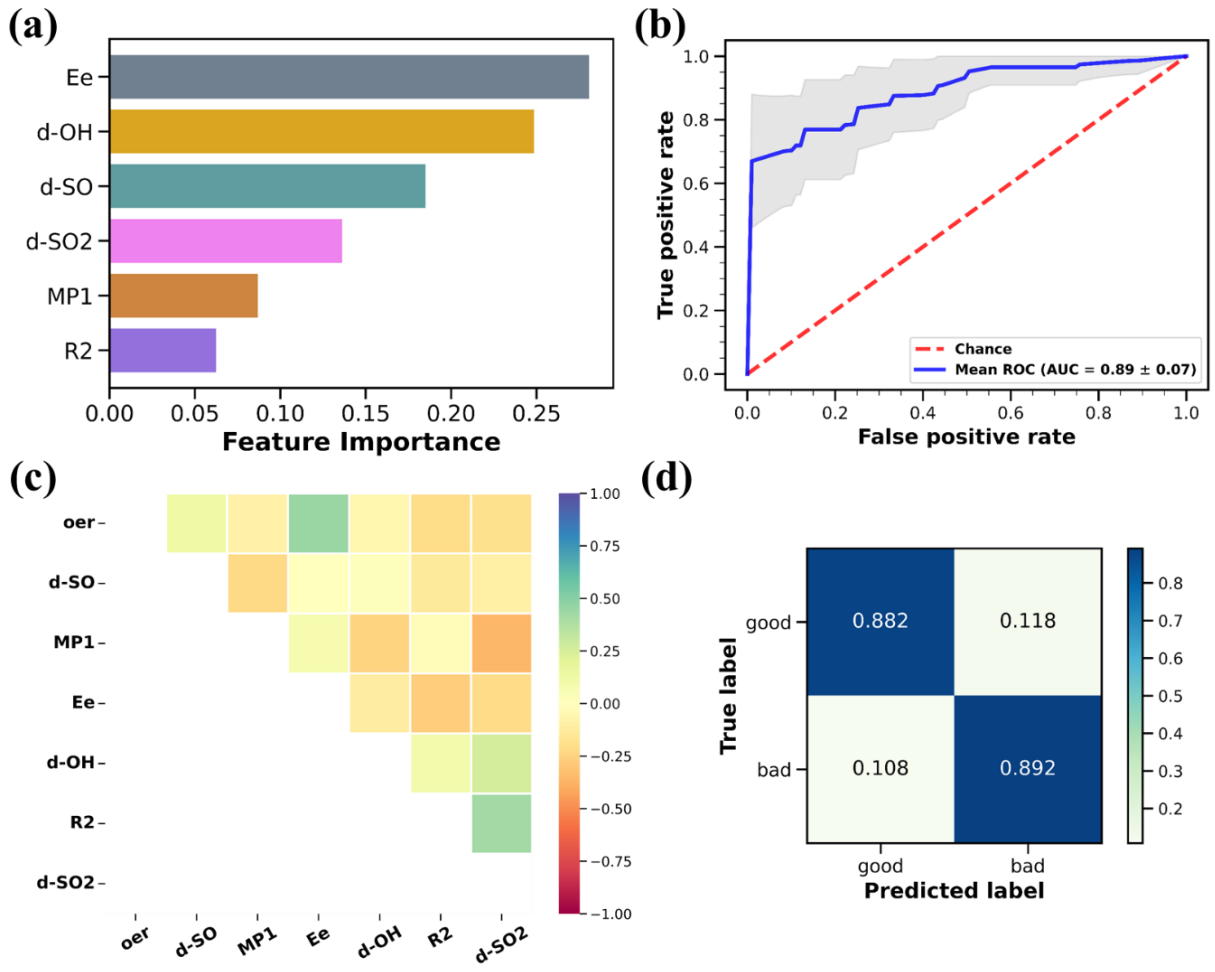

Fig. S9 Machine learning prediction of best explored classifier for OER activity on MXene combinations. **a)** Feature importance of reduced features. **b)** Mean ROC-AUC curve for Bagging classifier, the high AUC indicates the capability to distinguish between classes. **c)** Pearson feature-feature and feature-target correlation map. **d)** Normalized confusion matrix showing the great prediction level.

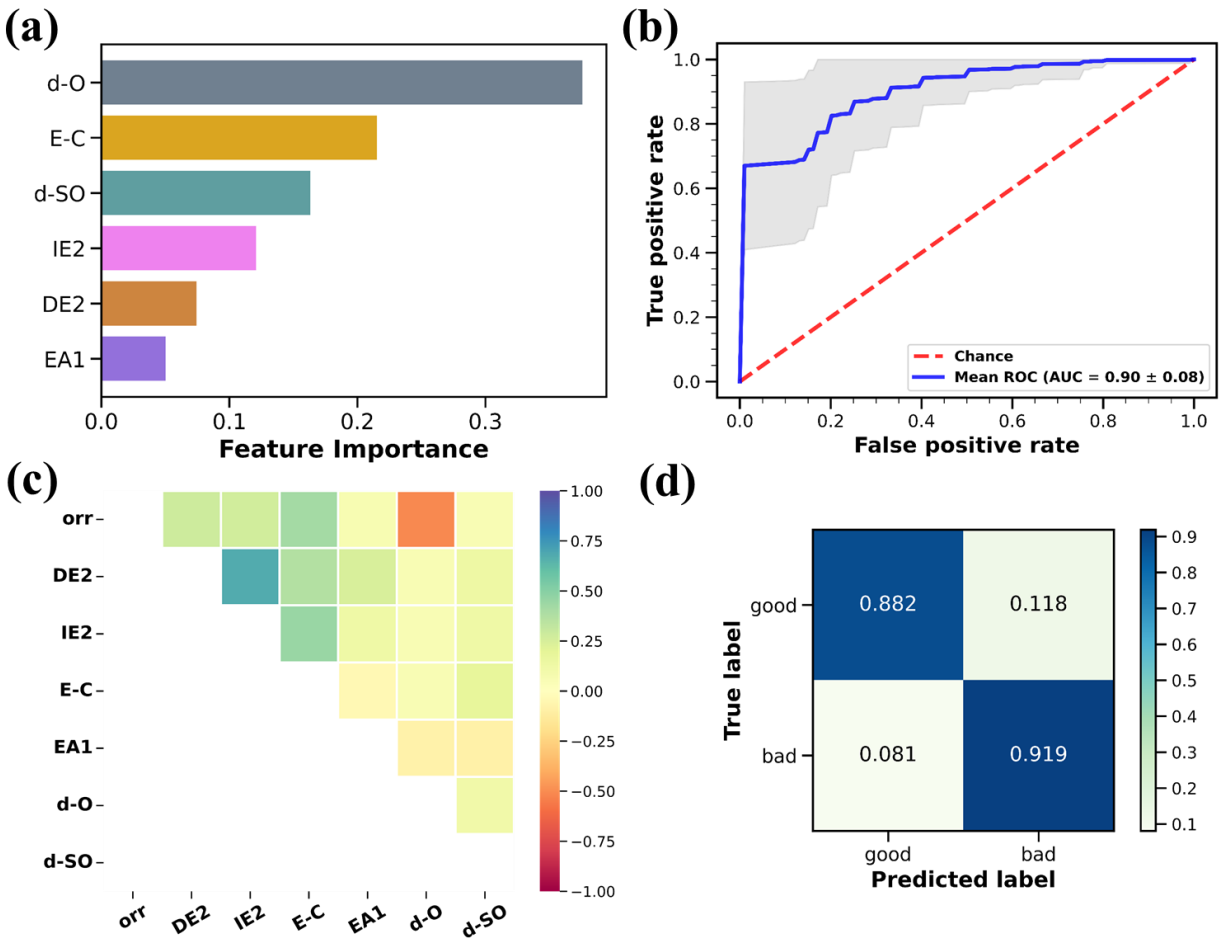

Fig. S10 Machine learning prediction of best explored classifier for ORR activity on MXene combinations. **a)** Feature importance of reduced features. **b)** Mean ROC-AUC curve for Random Forest classifier, the high AUC indicates the capability to distinguish between classes. **c)** Pearson feature-feature and feature-target correlation map. **d)** Normalized confusion matrix showing the great prediction level.

Supplementary Tables:

Table S1 Embedding energies (E_e in eV) for O-terminated MXenes with anchored TM atom (Ni/Fe/Cu) for all screened MXene combinations.

Anchored Metal	MXenes	E_e	MXenes	E_e	MXenes	E_e
Ni	Sc_2CrC_2	-4.10	Cr_2MoC_2	-4.64	Sc_2WN_2	-3.49
	Sc_2HfC_2	-4.64	Cr_2WC_2	-4.62	V_2CrN_2	-3.94
	Ti_2ScC_2	-5.08	Y_2NbC_2	-4.46	Cr_2VN_2	-4.31
	V_2ScC_2	-4.61	Zr_2ScC_2	-4.34	Cr_2NbN_2	-4.59
	V_2MoC_2	-4.20	Hf_2ScC_2	-4.17	Cr_2HfN_2	-4.19
	V_2TaC_2	-4.38	Sc_2TiN_2	-3.67	Y_2ScN_2	-5.81
	V_2WC_2	-4.14	Sc_2VN_2	-4.37	Mo_2TaN_2	-3.89
	Cr_2ScC_2	-5.69	Sc_2YN_2	-6.21		
	Cr_2VC_2	-4.61	Sc_2MoN_2	-4.51		
	Cr_2NbC_2	-4.80	Sc_2TaN_2	-3.51		
Fe	Sc_2CrC_2	-4.13	Cr_2MoC_2	-4.86	Sc_2WN_2	-3.79
	Sc_2HfC_2	-4.91	Cr_2WC_2	-4.84	V_2CrN_2	-3.97
	Ti_2ScC_2	-4.02	Y_2NbC_2	-4.51	Cr_2VN_2	-4.01
	V_2ScC_2	-4.57	Zr_2ScC_2	-4.35	Cr_2NbN_2	-4.71
	V_2MoC_2	-4.08	Hf_2ScC_2	-4.94	Cr_2HfN_2	-4.20
	V_2TaC_2	-4.44	Sc_2TiN_2	-4.25	Y_2ScN_2	-6.29
	V_2WC_2	-4.30	Sc_2VN_2	-4.81	Mo_2TaN_2	-4.37
	Cr_2ScC_2	-6.05	Sc_2YN_2	-6.85		
	Cr_2VC_2	-4.63	Sc_2MoN_2	-4.58		
	Cr_2NbC_2	-4.97	Sc_2TaN_2	-4.18		
Cu	Sc_2CrC_2	-3.29	Cr_2MoC_2	-2.92	Sc_2WN_2	-2.12
	Sc_2HfC_2	-3.08	Cr_2WC_2	-2.93	V_2CrN_2	-2.41
	Ti_2ScC_2	-2.92	Y_2NbC_2	-2.82	Cr_2VN_2	-2.68
	V_2ScC_2	-2.57	Zr_2ScC_2	-2.61	Cr_2NbN_2	-3.04
	V_2MoC_2	-2.26	Hf_2ScC_2	-2.90	Cr_2HfN_2	-2.66
	V_2TaC_2	-2.54	Sc_2TiN_2	-2.33	Y_2ScN_2	-3.69
	V_2WC_2	-2.21	Sc_2VN_2	-3.00	Mo_2TaN_2	-2.95
	Cr_2ScC_2	-3.48	Sc_2YN_2	-4.01		
	Cr_2VC_2	-2.90	Sc_2MoN_2	-3.43		
	Cr_2NbC_2	-2.71	Sc_2TaN_2	-2.25		

Table S2 $E_{e-c} = E_e - E_c$ (difference between embedding and cohesive energy in eV) for O-terminated MXene combinations with an anchored TM atom of Ni/Fe/Cu.

Anchored Metal	MXenes	E_{e-c}	MXenes	E_{e-c}	MXenes	E_{e-c}
Ni	Sc_2CrC_2	1.08	Cr_2MoC_2	0.54	Sc_2WN_2	1.69
	Sc_2HfC_2	0.54	Cr_2WC_2	0.56	V_2CrN_2	1.24
	Ti_2ScC_2	0.10	Y_2NbC_2	0.72	Cr_2VN_2	0.87
	V_2ScC_2	0.57	Zr_2ScC_2	0.84	Cr_2NbN_2	0.59
	V_2MoC_2	0.98	Hf_2ScC_2	1.01	Cr_2HfN_2	0.99
	V_2TaC_2	0.80	Sc_2TiN_2	1.51	Y_2ScN_2	-0.63
	V_2WC_2	1.04	Sc_2VN_2	0.81	Mo_2TaN_2	1.29
	Cr_2ScC_2	-0.51	Sc_2YN_2	-1.03		
	Cr_2VC_2	0.57	Sc_2MoN_2	0.67		
	Cr_2NbC_2	0.38	Sc_2TaN_2	1.67		
Fe	Sc_2CrC_2	1.14	Cr_2MoC_2	0.41	Sc_2WN_2	1.48
	Sc_2HfC_2	0.36	Cr_2WC_2	0.43	V_2CrN_2	1.30
	Ti_2ScC_2	1.25	Y_2NbC_2	0.76	Cr_2VN_2	1.26
	V_2ScC_2	0.70	Zr_2ScC_2	0.92	Cr_2NbN_2	0.56
	V_2MoC_2	1.19	Hf_2ScC_2	0.33	Cr_2HfN_2	1.07
	V_2TaC_2	0.83	Sc_2TiN_2	1.02	Y_2ScN_2	-1.02
	V_2WC_2	0.97	Sc_2VN_2	0.76	Mo_2TaN_2	0.90
	Cr_2ScC_2	-0.78	Sc_2YN_2	-1.58		
	Cr_2VC_2	0.64	Sc_2MoN_2	0.69		
	Cr_2NbC_2	0.30	Sc_2TaN_2	1.09		
Cu	Sc_2CrC_2	0.19	Cr_2MoC_2	0.56	Sc_2WN_2	1.36
	Sc_2HfC_2	0.40	Cr_2WC_2	0.55	V_2CrN_2	1.07
	Ti_2ScC_2	0.56	Y_2NbC_2	0.66	Cr_2VN_2	0.80
	V_2ScC_2	0.91	Zr_2ScC_2	0.87	Cr_2NbN_2	0.44
	V_2MoC_2	1.22	Hf_2ScC_2	0.58	Cr_2HfN_2	0.82
	V_2TaC_2	0.94	Sc_2TiN_2	1.15	Y_2ScN_2	-0.21
	V_2WC_2	1.27	Sc_2VN_2	0.48	Mo_2TaN_2	0.53
	Cr_2ScC_2	0.004	Sc_2YN_2	-0.53		
	Cr_2VC_2	0.58	Sc_2MoN_2	0.05		
	Cr_2NbC_2	0.77	Sc_2TaN_2	1.23		

Table S3 Adsorption free energies (ΔG in eV) of intermediates (OH*, O*, and OOH*) for screened $M_2M'X_2O_2$ type MXenes.

MXenes	Ni			Fe			Cu		
	ΔG_{OH}^*	ΔG_O^*	ΔG_{OOH}^*	ΔG_{OH}^*	ΔG_O^*	ΔG_{OOH}^*	ΔG_{OH}^*	ΔG_O^*	ΔG_{OOH}^*
Sc_2CrC_2	-0.04	1.24	2.94	-0.59	0.82	2.56	0.62	2.29	3.39
Sc_2HfC_2	0.20	1.43	3.04	-0.26	1.65	3.13	0.81	2.67	3.55
Ti_2ScC_2	0.77	1.79	3.36	-1.64	-0.03	1.50	0.75	3.01	3.48
V_2ScC_2	0.52	1.85	3.50	-0.29	1.15	2.93	0.33	2.74	3.24
V_2MoC_2	0.32	1.65	3.30	-0.33	0.85	2.67	0.26	2.07	3.22
V_2TaC_2	0.36	1.67	3.34	-0.33	1.11	2.82	0.36	2.20	3.28
V_2WC_2	0.35	1.66	3.36	1.07	0.83	2.63	0.17	2.07	3.19
Cr_2ScC_2	1.18	2.48	4.14	0.31	1.81	3.18	0.67	2.56	3.68
Cr_2VC_2	0.19	1.53	3.16	-0.41	1.04	2.74	0.51	2.56	3.38
Cr_2NbC_2	0.35	1.67	3.22	-0.27	1.18	2.88	0.60	2.61	3.45
Cr_2MoC_2	0.02	1.55	2.99	-0.29	1.09	2.89	0.49	2.36	3.38
Cr_2WC_2	0.20	1.55	3.14	-0.34	1.11	2.80	0.57	2.47	3.47
Y_2NbC_2	1.54	1.62	3.29	-0.27	1.28	2.87	0.58	3.24	3.42
Zr_2ScC_2	0.97	1.51	3.13	1.27	1.16	2.89	0.51	2.80	3.45
Hf_2ScC_2	0.32	1.73	3.29	-0.35	1.10	2.80	0.43	2.18	3.38
Sc_2TiN_2	-0.04	1.27	2.94	-0.61	0.75	2.53	0.25	2.49	3.26
Sc_2VN_2	0.42	1.39	2.98	-0.55	0.92	2.59	0.42	2.54	3.30
Sc_2YN_2	0.75	2.19	3.64	0.20	1.57	3.25	1.06	2.90	3.84
Sc_2MoN_2	-0.02	1.31	2.96	-0.61	0.76	2.53	0.74	2.18	3.29
Sc_2TaN_2	-0.08	1.19	2.90	-0.58	0.74	2.57	0.19	2.50	3.18
Sc_2WN_2	-0.03	1.24	2.96	-0.79	0.48	2.35	0.74	2.40	3.08
V_2CrN_2	-0.06	1.23	2.32	-0.52	0.83	2.04	0.41	2.44	2.78
Cr_2VN_2	0.04	1.48	3.07	-0.50	0.93	2.64	0.47	2.45	3.46
Cr_2NbN_2	0.10	1.49	3.11	-0.47	0.99	2.67	0.55	2.62	3.37
Cr_2HfN_2	0.20	1.47	3.16	-0.36	1.11	2.66	0.49	2.56	3.47
Y_2ScN_2	0.77	2.16	3.68	0.04	1.62	3.33	1.00	2.90	3.81
Mo_2TaN_2	-0.12	1.21	2.85	-	-	-	0.61	2.30	3.43

Table S4 Theoretical overpotentials for OER (η^{OER} in V) of doped $M_2M'X_2O_2$ type MXene combinations.

MXenes	Ni	Fe	Cu
	η^{OER}	η^{OER}	η^{OER}
Sc_2CrC_2	0.75	1.13	0.44
Sc_2HfC_2	0.65	0.67	0.63
Ti_2ScC_2	0.33	2.19	1.03
V_2ScC_2	0.43	0.76	1.17
V_2MoC_2	0.42	1.02	0.58
V_2TaC_2	0.44	0.87	0.61
V_2WC_2	0.47	1.06	0.68
Cr_2ScC_2	0.43	0.51	0.66
Cr_2VC_2	0.53	0.95	0.82
Cr_2NbC_2	0.47	0.81	0.78
Cr_2MoC_2	0.70	0.80	0.64
Cr_2WC_2	0.55	0.89	0.68
Y_2NbC_2	0.45	0.82	1.43
Zr_2ScC_2	0.56	0.80	1.06
Hf_2ScC_2	0.40	0.89	0.52
Sc_2TiN_2	0.75	1.16	1.02
Sc_2VN_2	0.71	1.10	0.90
Sc_2YN_2	0.22	0.45	0.61
Sc_2MoN_2	0.73	1.16	0.40
Sc_2TaN_2	0.79	1.12	1.09
Sc_2WN_2	0.73	1.34	0.61
V_2CrN_2	1.37	1.65	0.91
Cr_2VN_2	0.62	1.05	0.75
Cr_2NbN_2	0.58	1.02	0.83
Cr_2HfN_2	0.53	1.03	0.84
Y_2ScN_2	0.29	0.48	0.66
Mo_2TaN_2	0.84	-	0.46

Table S5 Theoretical overpotentials for ORR (η^{ORR} in V) of doped $M_2M'X_2O_2$ type MXene combinations.

MXenes	Ni	Fe	Cu
	η^{ORR}	η^{ORR}	η^{ORR}
Sc_2CrC_2	1.27	1.82	0.61
Sc_2HfC_2	1.03	1.49	0.42
Ti_2ScC_2	0.46	2.87	0.76
V_2ScC_2	0.71	1.52	0.90
V_2MoC_2	0.91	1.56	0.97
V_2TaC_2	0.87	1.56	0.87
V_2WC_2	0.88	1.47	1.06
Cr_2ScC_2	0.45	0.92	0.56
Cr_2VC_2	1.04	1.64	0.72
Cr_2NbC_2	0.88	1.50	0.63
Cr_2MoC_2	1.21	1.52	0.74
Cr_2WC_2	1.03	1.57	0.66
Y_2NbC_2	1.15	1.50	1.04
Zr_2ScC_2	0.69	1.34	0.72
Hf_2ScC_2	0.91	1.58	0.80
Sc_2TiN_2	1.27	1.84	0.98
Sc_2VN_2	0.81	1.78	0.81
Sc_2YN_2	0.48	1.03	0.28
Sc_2MoN_2	1.25	1.84	0.49
Sc_2TaN_2	1.31	1.81	1.04
Sc_2WN_2	1.26	2.02	0.55
V_2CrN_2	1.29	1.75	0.88
Cr_2VN_2	1.19	1.73	0.76
Cr_2NbN_2	1.13	1.70	0.68
Cr_2HfN_2	1.03	1.59	0.74
Y_2ScN_2	0.46	1.19	0.31
Mo_2TaN_2	1.35	-	0.62

Table S6 Hydrogen adsorption free energies (ΔG_{H^*} in eV) for doped $M_2M'X_2O_2$ type MXene combinations.

MXenes	Ni	Fe	Cu
	ΔG_{H^*}	ΔG_{H^*}	ΔG_{H^*}
Sc_2CrC_2	0.05	0.09	0.04
Sc_2HfC_2	-0.86	0.91	-0.76
Ti_2ScC_2	-0.29	-1.86	-0.50
V_2ScC_2	-0.11	-0.20	-0.28
V_2MoC_2	0.10	-0.02	0.02
V_2TaC_2	-0.27	-0.17	-0.20
V_2WC_2	-0.07	0.01	-0.01
Cr_2ScC_2	-0.08	-0.07	-0.35
Cr_2VC_2	-0.31	-0.24	-0.34
Cr_2NbC_2	-0.62	-0.42	-0.55
Cr_2MoC_2	-0.26	-0.17	-0.32
Cr_2WC_2	-0.39	-0.25	-0.30
Y_2NbC_2	-0.37	-0.35	-0.38
Zr_2ScC_2	-0.29	-0.30	-0.29
Hf_2ScC_2	-0.22	-0.21	-0.20
Sc_2TiN_2	0.21	0.27	0.26
Sc_2VN_2	-0.01	0.13	-0.04
Sc_2YN_2	-1.24	-1.18	-1.34
Sc_2MoN_2	0.34	0.36	0.22
Sc_2TaN_2	0.15	0.34	0.26
Sc_2WN_2	0.90	0.62	0.62
V_2CrN_2	0.12	0.17	0.08
Cr_2VN_2	-0.03	0.00	-0.10
Cr_2NbN_2	-0.06	-0.17	-0.12
Cr_2HfN_2	-0.12	-0.10	-0.22
Y_2ScN_2	-1.12	-1.06	-1.15
Mo_2TaN_2	0.10	0.32	0.48

Table S7 Reaction free energies (eV) of elementary steps for OER in Ni-doped $M_2M'X_2O_2$ type MXene combinations.

MXenes	ΔG_1	ΔG_2	ΔG_3	ΔG_4
Sc_2CrC_2	-0.04	1.28	1.70	1.98
Sc_2HfC_2	0.20	1.22	1.62	1.88
Ti_2ScC_2	0.77	1.03	1.56	1.56
V_2ScC_2	0.52	1.33	1.66	1.42
V_2MoC_2	0.32	1.33	1.65	1.62
V_2TaC_2	0.36	1.31	1.67	1.58
V_2WC_2	0.35	1.30	1.70	1.56
Cr_2ScC_2	1.18	1.29	1.66	0.78
Cr_2VC_2	0.19	1.33	1.64	1.76
Cr_2NbC_2	0.35	1.32	1.54	1.70
Cr_2MoC_2	0.02	1.53	1.45	1.93
Cr_2WC_2	0.20	1.35	1.59	1.78
Y_2NbC_2	1.54	0.08	1.68	1.63
Zr_2ScC_2	0.97	0.54	1.63	1.79
Hf_2ScC_2	0.32	1.41	1.57	1.63
Sc_2TiN_2	-0.04	1.30	1.68	1.98
Sc_2VN_2	0.42	0.97	1.59	1.94
Sc_2YN_2	0.75	1.44	1.45	1.28
Sc_2MoN_2	-0.02	1.33	1.65	1.96
Sc_2TaN_2	-0.08	1.27	1.72	2.02
Sc_2WN_2	-0.03	1.27	1.72	1.96
V_2CrN_2	-0.06	1.29	1.09	2.60
Cr_2VN_2	0.04	1.44	1.59	1.85
Cr_2NbN_2	0.10	1.39	1.62	1.81
Cr_2HfN_2	0.20	1.27	1.69	1.76
Y_2ScN_2	0.77	1.39	1.52	1.24
Mo_2TaN_2	-0.12	1.32	1.65	2.07

Table S8 Reaction free energies (eV) of elementary steps for OER in Fe-doped $M_2M'X_2O_2$ type MXene combinations.

MXenes	ΔG_1	ΔG_2	ΔG_3	ΔG_4
Sc_2CrC_2	-0.59	1.40	1.74	2.36
Sc_2HfC_2	-0.26	1.90	1.49	1.79
Ti_2ScC_2	-1.64	1.62	1.52	3.42
V_2ScC_2	-0.29	1.44	1.78	1.99
V_2MoC_2	-0.33	1.17	1.82	2.25
V_2TaC_2	-0.33	1.44	1.71	2.10
V_2WC_2	1.07	-0.24	1.80	2.29
Cr_2ScC_2	0.31	1.50	1.38	1.74
Cr_2VC_2	-0.41	1.44	1.70	2.18
Cr_2NbC_2	-0.27	1.45	1.70	2.04
Cr_2MoC_2	-0.29	1.37	1.81	2.03
Cr_2WC_2	-0.34	1.45	1.70	2.12
Y_2NbC_2	-0.27	1.55	1.59	2.05
Zr_2ScC_2	1.27	-0.11	1.73	2.03
Hf_2ScC_2	-0.35	1.45	1.70	2.12
Sc_2TiN_2	-0.61	1.36	1.79	2.39
Sc_2VN_2	-0.55	1.47	1.67	2.33
Sc_2YN_2	0.20	1.37	1.68	1.67
Sc_2MoN_2	-0.61	1.38	1.77	2.39
Sc_2TaN_2	-0.58	1.32	1.83	2.35
Sc_2WN_2	-0.79	1.27	1.88	2.57
V_2CrN_2	-0.52	1.35	1.21	2.88
Cr_2VN_2	-0.50	1.43	1.71	2.28
Cr_2NbN_2	-0.47	1.46	1.69	2.25
Cr_2HfN_2	-0.36	1.48	1.55	2.26
Y_2ScN_2	0.04	1.58	1.71	1.59
Mo_2TaN_2	-	-	-	-

Table S9 Reaction free energies (eV) of elementary steps for OER in Cu-doped $M_2M'X_2O_2$ type MXene combinations.

MXenes	ΔG_1	ΔG_2	ΔG_3	ΔG_4
Sc_2CrC_2	0.62	1.67	1.10	1.53
Sc_2HfC_2	0.81	1.86	0.88	1.37
Ti_2ScC_2	0.75	2.26	0.47	1.44
V_2ScC_2	0.33	2.40	0.50	1.68
V_2MoC_2	0.26	1.81	1.15	1.70
V_2TaC_2	0.36	1.84	1.08	1.64
V_2WC_2	0.17	1.91	1.12	1.73
Cr_2ScC_2	0.67	1.89	1.12	1.24
Cr_2VC_2	0.51	2.05	0.82	1.54
Cr_2NbC_2	0.60	2.01	0.84	1.47
Cr_2MoC_2	0.49	1.87	1.02	1.54
Cr_2WC_2	0.57	1.91	1.00	1.45
Y_2NbC_2	0.58	2.66	0.19	1.50
Zr_2ScC_2	0.51	2.29	0.66	1.47
Hf_2ScC_2	0.43	1.75	1.20	1.54
Sc_2TiN_2	0.25	2.25	0.77	1.66
Sc_2VN_2	0.42	2.13	0.75	1.62
Sc_2YN_2	1.05	1.84	0.95	1.08
Sc_2MoN_2	0.74	1.45	1.11	1.63
Sc_2TaN_2	0.19	2.32	0.68	1.74
Sc_2WN_2	0.74	1.65	0.68	1.84
V_2CrN_2	0.41	2.03	0.35	2.14
Cr_2VN_2	0.47	1.98	1.01	1.46
Cr_2NbN_2	0.55	2.06	0.76	1.55
Cr_2HfN_2	0.49	2.07	0.92	1.45
Y_2ScN_2	1.00	1.89	0.92	1.11
Mo_2TaN_2	0.61	1.69	1.13	1.49

Table S10 Reaction free energies (eV) of elementary steps for ORR in Ni-doped $M_2M'X_2O_2$ type MXene combinations.

MXenes	ΔG_1	ΔG_2	ΔG_3	ΔG_4
Sc_2CrC_2	-1.98	-1.70	-1.28	0.04
Sc_2HfC_2	-1.88	-1.62	-1.22	-0.20
Ti_2ScC_2	-1.56	-1.56	-1.03	-0.77
V_2ScC_2	-1.42	-1.66	-1.33	-0.52
V_2MoC_2	-1.62	-1.65	-1.33	-0.32
V_2TaC_2	-1.58	-1.67	-1.31	-0.36
V_2WC_2	-1.56	-1.70	-1.30	-0.35
Cr_2ScC_2	-0.78	-1.66	-1.29	-1.18
Cr_2VC_2	-1.76	-1.64	-1.33	-0.19
Cr_2NbC_2	-1.70	-1.54	-1.32	-0.35
Cr_2MoC_2	-1.93	-1.45	-1.53	-0.02
Cr_2WC_2	-1.78	-1.59	-1.35	-0.20
Y_2NbC_2	-1.63	-1.68	-0.08	-1.54
Zr_2ScC_2	-1.79	-1.63	-0.54	-0.97
Hf_2ScC_2	-1.63	-1.57	-1.41	-0.32
Sc_2TiN_2	-1.98	-1.68	-1.30	0.04
Sc_2VN_2	-1.94	-1.59	-0.97	-0.42
Sc_2YN_2	-1.28	-1.45	-1.44	-0.75
Sc_2MoN_2	-1.96	-1.65	-1.33	0.02
Sc_2TaN_2	-2.02	-1.72	-1.27	0.08
Sc_2WN_2	-1.96	-1.72	-1.27	0.03
V_2CrN_2	-2.60	-1.09	-1.29	0.06
Cr_2VN_2	-1.85	-1.59	-1.44	-0.04
Cr_2NbN_2	-1.81	-1.62	-1.39	-0.10
Cr_2HfN_2	-1.76	-1.69	-1.27	-0.20
Y_2ScN_2	-1.24	-1.52	-1.39	-0.77
Mo_2TaN_2	-2.07	-1.65	-1.32	0.12

Table S11 Reaction free energies (eV) of elementary steps for ORR in Fe-doped $M_2M'X_2O_2$ type MXene combinations.

MXenes	ΔG_1	ΔG_2	ΔG_3	ΔG_4
Sc_2CrC_2	-2.36	-1.74	-1.40	0.59
Sc_2HfC_2	-1.79	-1.49	-1.90	0.26
Ti_2ScC_2	-3.42	-1.52	-1.62	1.64
V_2ScC_2	-1.99	-1.78	-1.44	0.29
V_2MoC_2	-2.25	-1.82	-1.17	0.33
V_2TaC_2	-2.10	-1.71	-1.44	0.33
V_2WC_2	-2.29	-1.80	0.24	-1.07
Cr_2ScC_2	-1.74	-1.38	-1.50	-0.31
Cr_2VC_2	-2.18	-1.70	-1.44	0.41
Cr_2NbC_2	-2.04	-1.70	-1.45	0.27
Cr_2MoC_2	-2.03	-1.81	-1.37	0.29
Cr_2WC_2	-2.12	-1.70	-1.45	0.34
Y_2NbC_2	-2.05	-1.59	-1.55	0.27
Zr_2ScC_2	-2.03	-1.73	0.11	-1.27
Hf_2ScC_2	-2.12	-1.70	-1.45	0.35
Sc_2TiN_2	-2.39	-1.79	-1.36	0.61
Sc_2VN_2	-2.33	-1.67	-1.47	0.55
Sc_2YN_2	-1.67	-1.68	-1.37	-0.20
Sc_2MoN_2	-2.39	-1.77	-1.38	0.61
Sc_2TaN_2	-2.35	-1.83	-1.32	0.58
Sc_2WN_2	-2.57	-1.88	-1.27	0.79
V_2CrN_2	-2.88	-1.21	-1.35	0.52
Cr_2VN_2	-2.28	-1.71	-1.43	0.50
Cr_2NbN_2	-2.25	-1.69	-1.46	0.47
Cr_2HfN_2	-2.26	-1.55	-1.48	0.36
Y_2ScN_2	-1.59	-1.71	-1.58	-0.04
Mo_2TaN_2	-	-	-	-

Table S12 Reaction free energies (eV) of elementary steps for ORR in Cu-doped $M_2M'X_2O_2$ type MXene combinations.

MXenes	ΔG_1	ΔG_2	ΔG_3	ΔG_4
Sc_2CrC_2	-1.53	-1.10	-1.67	-0.62
Sc_2HfC_2	-1.37	-0.88	-1.86	-0.81
Ti_2ScC_2	-1.44	-0.47	-2.26	-0.75
V_2ScC_2	-1.68	-0.50	-2.40	-0.33
V_2MoC_2	-1.70	-1.15	-1.81	-0.26
V_2TaC_2	-1.64	-1.08	-1.84	-0.36
V_2WC_2	-1.73	-1.12	-1.91	-0.17
Cr_2ScC_2	-1.24	-1.12	-1.89	-0.67
Cr_2VC_2	-1.54	-0.82	-2.05	-0.51
Cr_2NbC_2	-1.47	-0.84	-2.01	-0.60
Cr_2MoC_2	-1.54	-1.02	-1.87	-0.49
Cr_2WC_2	-1.45	-1.00	-1.91	-0.57
Y_2NbC_2	-1.50	-0.19	-2.66	-0.58
Zr_2ScC_2	-1.47	-0.66	-2.29	-0.51
Hf_2ScC_2	-1.54	-1.20	-1.75	-0.43
Sc_2TiN_2	-1.66	-0.77	-2.25	-0.25
Sc_2VN_2	-1.62	-0.75	-2.13	-0.42
Sc_2YN_2	-1.08	-0.95	-1.84	-1.05
Sc_2MoN_2	-1.63	-1.11	-1.45	-0.74
Sc_2TaN_2	-1.74	-0.68	-2.32	-0.19
Sc_2WN_2	-1.84	-0.68	-1.65	-0.74
V_2CrN_2	-2.14	-0.35	-2.03	-0.41
Cr_2VN_2	-1.46	-1.01	-1.98	-0.47
Cr_2NbN_2	-1.55	-0.76	-2.06	-0.55
Cr_2HfN_2	-1.45	-0.92	-2.07	-0.49
Y_2ScN_2	-1.11	-0.92	-1.89	-1.00
Mo_2TaN_2	-1.49	-1.13	-1.69	-0.61

Table S13 The difference between zero-point energy changes (ΔZPE) and entropic energy contributions (TΔS) in eV for all intermediates at 298.15K.

	ΔZPE-TΔS
Pristine	0
OH*	0.26
O*	-0.075
OOH*	0.206
H*	0.26
0.5 H_2	-0.06
H_2O	-0.1

Table S14 Overpotentials of efficient OER and ORR (η^{OER} in V) catalysts for MXenes with the solvent effect (dielectric constant : 80). The results in the absence of solvent effect are in parentheses.

MXenes	η^{OER}	η^{ORR}
Ni-$Sc_2YN_2O_2$	0.25 (0.22)	0.41 (0.48)
Ni-$Ti_2ScC_2O_2$	0.27 (0.33)	0.48 (0.46)
Ni-$Y_2ScN_2O_2$	0.24 (0.29)	0.40 (0.46)
Ni-$Cr_2ScC_2O_2$	0.45 (0.43)	0.42 (0.45)
Cu-$Sc_2MoN_2O_2$	0.44 (0.40)	0.57 (0.49)
Cu-$Sc_2CrC_2O_2$	0.41 (0.44)	0.53 (0.61)

Table S15 ΔG_{H^*} (eV) for HER in the presence of solvent effect for most efficient MXenes with $|\Delta G_{H^*}| \leq 0.02$ eV. The results in the absence of solvent effect are in parentheses.

MXenes	HER ($\|\Delta G_{H^*}\|$)
Fe-$Cr_2VN_2O_2$	0.017 (0.004)
Fe-$V_2WC_2O_2$	0.015 (0.007)
Ni-$Sc_2VN_2O_2$	0.009 (0.007)
Cu-$V_2WC_2O_2$	0.025 (0.013)
Cu-$V_2MoC_2O_2$	0.015 (0.017)
Fe-$V_2MoC_2O_2$	0.039 (0.019)

Table S16 The Bader charge transfer (e^-/atom) from doped TM to adsorbed O atom for O* intermediate of efficient bifunctional catalysts. The negative and positive signs indicate the gain and loss of charge, respectively.

MXenes	O*	Doped-TM
Ni-$Sc_2YN_2O_2$	-0.509	1.08
Ni-$Ti_2ScC_2O_2$	-0.610	1.99
Ni-$Y_2ScN_2O_2$	-0.508	1.14
Ni-$Cr_2ScC_2O_2$	-0.445	1.17
Cu-$Sc_2MoN_2O_2$	-0.490	0.84

Table S17 Hydrogen adsorption energies ($E_{ad} = E_{Mx+H} – E_{Mx} - E_H$ in eV) for Ni-doped $M_2M'X_2O_2$ type MXene combinations. The considered sites are S1, S2, and S3.

MXenes	Ni-doped		
	S1	**S2**	**S3**
Sc_2CrC_2	0.24	0.18	-0.31
Sc_2HfC_2	-1.01	-0.96	-1.22
Ti_2ScC_2	-0.44	0.93	-0.65
V_2ScC_2	-0.41	0.64	-0.48
V_2MoC_2	-0.07	0.69	-0.26
V_2TaC_2	-0.38	2.65	-0.64
V_2WC_2	-0.04	0.22	-0.43
Cr_2ScC_2	-0.81	0.75	-0.65
Cr_2VC_2	-0.55	0.54	-0.68
Cr_2NbC_2	-0.88	0.29	-0.99
Cr_2MoC_2	-0.58	-	-0.62
Cr_2WC_2	-0.69	0.60	-0.76
Y_2NbC_2	-0.34	0.75	-0.73
Zr_2ScC_2	-0.43	-	-0.66
Hf_2ScC_2	-0.23	-	-0.58
Sc_2TiN_2	0.14	1.02	-0.15
Sc_2VN_2	-0.01	0.34	-0.37
Sc_2YN_2	-0.96	1.13	-1.61
Sc_2MoN_2	0.11	-	-0.02
Sc_2TaN_2	0.10	1.56	-0.22
Sc_2WN_2	0.56	-	0.54
V_2CrN_2	-0.20	0.25	-0.25
Cr_2VN_2	-0.33	0.45	-0.39
Cr_2NbN_2	-0.12	0.67	-0.43
Cr_2HfN_2	-0.29	0.06	-0.48
Y_2ScN_2	-0.77	-	-1.48
Mo_2TaN_2	-0.12	0.74	-0.27

"-" denotes the unstable intermediate.